Published in final edited form as:

Mol Cancer Ther. 2016 September ; 15(9): 2187–2197. doi:10.1158/1535-7163.MCT-15-0427.

Periostin (POSTN) regulates tumor resistance to antiangiogenic therapy in glioma models

Soon Young Park[1], **Yuji Piao**[1], **Kang Jin Jeong**[2], **Jianwen Dong**[1], and **John F. de Groot**[1]

[1]Department of Neuro-Oncology, The University of Texas MD Anderson Cancer Center, Houston, Texas, USA

[2]Department of Systems Biology, The University of Texas MD Anderson Cancer Center, Houston, Texas, USA

Abstract

Periostin (POSTN) interacts with multiple integrins to coordinate a variety of cellular processes, including epithelial-to-mesenchymal transition (EMT) and cell migration. In our previous study, anti-vascular endothelial growth factor A (VEGF-A) therapy was associated with resistance and EMT. The present study sought to determine the role of POSTN in the resistance of glioma stem cells (GSCs) to antiangiogenic therapy. In mouse xenograft models of human glioma, POSTN expression was associated with acquired resistance to anti-VEGF-A therapy and had a synergistic effect with bevacizumab in prolonging survival and decreasing tumor volume. Resistance to anti-VEGF-A therapy regulated by POSTN was associated with increased expression of transforming growth factor beta-1 (TGF beta1) and hypoxia-inducible factor-1 alpha (HIF1 alpha) in GSCs. At the molecular level, POSTN regulated invasion and expression of EMT (caveolin-1) and angiogenesis-related genes (HIF1 alpha and VEGF-A) through activation of signal transducer and activator of transcription 3 (STAT3). Moreover, recombinant POSTN increased GSC invasion. Collectively, our findings suggest that POSTN plays an important role in glioma invasion and resistance to antiangiogenic therapy.

Keywords

POSTN; Glioma; VEGF-A; Invasion; Resistance

Introduction

Tumor angiogenesis is regulated by angiogenic factors, including vascular endothelial growth factor (VEGF), platelet-derived growth factor, and HIF1 alpha (1). The transcription factor HIF1 alpha plays a critical role in regulation of VEGF stabilization during hypoxia (2). Glioma stem cells (GSCs) increase tumor angiogenesis via elevated secretion of VEGF-A (3). The production of VEGF in gliomas is significant, with researchers finding VEGF

Address correspondence to: John de Groot, Department of Neuro-Oncology, Unit 431, The University of Texas MD Anderson Cancer Center, 1515 Holcombe Boulevard, Houston, TX 77030, USA. Phone: 713.745.3072; Fax: 713.794.4999; jdegroot@mdanderson.org.

Disclosure of Potential Conflicts of Interest: John de Groot reports serving on an advisory board for Genentech/Roche. The other authors declare no conflict of interest.

levels 200- to 300-fold higher in cystic fluid than in serum in glioblastoma (GBM) patients (4). GBM is the most malignant brain tumor and is highly resistant to intensive combination therapies (5). Furthermore, GBMs are highly vascularized tumors, and high microvessel densities in gliomas are highly correlated with poor prognosis (6). Proliferation of endothelial cells is observed frequently and exclusively in mesenchymal type GBMs, correlating with poor prognosis (7). Bevacizumab is a humanized recombinant monoclonal antibody against VEGF-A that is composed of human IgG1 constant and murine VEGF-binding regions (8). Studies of antiangiogenic therapies in xenograft mouse models of human GBM encouraged clinical studies of anti-VEGF-A antibodies (9). Resistance of glioma to anti-VEGF-A therapy is associated with the EMT (10). Besides their roles in tumor cell invasion, these alternative neovascularization mechanisms may contribute to resistance of GBM to antiangiogenic therapies (5).

Periostin (POSTN; osteoblast-specific factor 2) is a 90-kDa extracellular matrix (ECM) protein containing an amino-terminal EMI domain, tandem repeats of four fasciclin domains, and a carboxy-terminal (C-terminal) domain, including a heparin-binding site (11). In humans, fasciclin I domains are found in βigh3 (12), stabilin (13), and POSTN (14). Stromal POSTN plays a key role in regulation of cancer stem cell maintenance and expansion during metastatic colonization (15). It was reported that POSTN functions as a progression-associated and prognostic biomarker in glioma cases via induction of an invasive and proliferative phenotype (16). In another study, POSTN mRNA expression was markedly higher in grade IV gliomas than in grade II and III tumors (17). POSTN interacts with several integrin receptors, such as αvβ1 and αvβ3, to regulate cellular responses such as cell proliferation, EMT, and cell migration (18). During EMT, POSTN can increase vimentin, fibronectin, and matrix metalloproteinase (MMP)-9 expression (19). Moreover, POSTN increases angiogenesis via VEGFR2 expression in endothelial cells (20), and upregulation of VEGF-C expression may promote lymphangiogenesis (21). POSTN is induced by transforming growth factor beta (TGF beta) (22) and BMP2 (23), which has been detected in glioma cell cultures and in cerebrospinal fluid and brain tumor biopsy samples from glioma patients (24). Also, GBMs release active TGF beta1 and TGF beta2 (25). Although POSTN is known to be important to glioma progression and to VEGF-A expression in other cancer cells, its role in these processes and its relationship to TGF beta are unclear. Our purpose here was to determine the relationship of POSTN to invasion and VEGF-A expression in GSCs and its role in response to VEGF-A therapy in *in vivo* glioma models.

Materials and Methods

Cell lines, reagents, and treatment

GSC lines were obtained from Drs. Howard Colman, Erik Sulman, and Frederick Lang (The University of Texas MD Anderson Cancer Center). GSC lines were isolated from fresh surgical specimens of human GBM and cultured as GBM neurospheres in neurosphere medium: Dulbecco modified Eagle medium–F12 medium (1:1) with added B27 (Invitrogen), basic fibroblast growth factor (bFGF; Sigma), and epidermal growth factor (EGF; Sigma) (26). Acquisition of these cell lines was approved by the Institutional Review Board of MD

Anderson Cancer Center and were obtained from 2005 to 2012. 293T embryonic kidney cells were obtained from the American Type Culture Collection (ATCC) and maintained in Dulbecco's modified Eagle medium (DMEM) (Sigma) supplemented with 10% fetal bovine serum (FBS). All cell lines were tested and authenticated by DNA typing at the MD Anderson Cancer Center Cell Line Characterization Core and were subsequently verified for our study (December 2014). GSC lines were reported previously (10). All cell lines were cultured early-passage at 37°C in a humidified atmosphere of 5% CO_2 and 95% air. All cell lines were free of mycoplasma contamination. Recombinant POSTN (cat. #3548-F2–050) and TGF beta1 (cat. #240-B-010) were purchased from R&D Systems.

Stable knockdown of POSTN in GSCs

293T cells were transfected with short hairpin RNA (shRNA) packaged with pMD2G and pCMVR8.74 DNA using PolyJet reagents (cat. #SL100688; Signagen) according to the vendor's instructions. Empty vector (pGIPZ control, cat. #RHS4349), POSTN shRNA1 (cat. #V3LHS_363450), and POSTN shRNA2 (cat. #V3LHS_363449) were purchased from GE Healthcare. Negative (scramble) shRNA was purchased from Sigma (cat. #SHC002). GSCs were infected with the 293T viral soup and selected with puromycin (1 μg/mL) for 7 days. Each well of a 96-well plate was seeded with a single cell, and the high-efficiency cells were selected for further analysis.

Animal xenografts

For the *in vivo* experiments, we used 4- to 6-week-old female nude mice strictly inbred at MD Anderson and maintained in the MD Anderson Research Animal Support Facility in accordance with Institute of Laboratory Animal Resources standards. The cells (5×10^5) were implanted intracranially into the nude mice as described previously (10). Four days after implantation, bevacizumab (Avastin [10 mg/kg]; Genentech) or vehicle was administered via intraperitoneal injection twice a week. The mice were killed at the indicated intervals, and their brains were removed and processed for analysis. Tumor volumes were calculated by the formula ([width] × [width] × [length])/2. The animal experiments were approved by the MD Anderson Institutional Animal Care and Use Committee.

Gene expression analysis

Total RNA was extracted from GSCs using an RNeasy Mini Kit coupled with DNase (QIAGEN) and reverse-transcribed using a High-Capacity cDNA Reverse Transcription Kit (Applied Biosystems). Gene expression was analyzed by using RT^2 Profiler polymerase chain reaction (PCR) arrays (SABiosciences) per the manufacturer's instructions. EMT (cat. PAHS-090Z) and angiogenesis (cat. PAHS-024Z) PCR arrays were used. Quantitative PCR was performed according to detection protocols recommended by SABiosciences. C_t values for a reaction set were analyzed online at the manufacturer's website.

Microarray

Fresh frozen tumor tissue (after implantation 7 weeks) was processed and total RNA extracted according to standard methods (QIAGEN) for transcriptome analysis using

Affymetrix GeneChipHuman GenomeHG-U133 Plus 2.0 Arrays (cat. #900466; Affymetrix). Quality of samples was confirmed and microarray processing were carried out by the MD Anderson Cancer Center Sequencing and Microarray Core Facility. The microarray data have been submitted to the Gene Expression Omnibus (GEO) public database at NCBI, accession number GSE73071.

Western blot analysis

GSCs were subjected to lysis in radio-immunoprecipitation assay lysis buffer (Cell Signaling Technology) containing proteinase (Sigma-Aldrich) and a phosphatase cocktail (Thermo Fisher Scientific). The protein concentration in each supernatant was determined by a bicinchoninic acid protein assay (Bio-Rad). Samples were subjected to sodium dodecyl sulfate–polyacrylamide gel separation, and the separated proteins were electrophoretically transferred to polyvinylidene fluoride membranes. Blots were incubated with the primary antibody overnight at 4°C and incubated with horseradish peroxidase–linked secondary anti-rabbit or anti-mouse antibody (Bio-Rad). Antibodies against signal transducer and activator of transcription 3 (STAT3; cat. #9139), phosphorylated STAT3 (Tyr705; cat. #9135), caveolin-1 (cat. #3238), N-cadherin (cat. #4061), SMAD2 (cat. #5339), SMAD3 (cat. #9523), phosphorylated SMAD2 (cat. #3108), and phosphorylated SMAD3 (cat. #9520) were purchased from Cell Signaling Technology. Other antibodies used for Western blotting were POSTN (cat. #AP11962b; Abgent); HIF1 alpha (cat. #610958; BD Biosciences); integrin β1 (cat. #18887), integrin β3 (cat. #6627), and GAPDH (cat. #32233; all, Santa Cruz Biotechnology); and α-tubulin (cat. #T9026; Sigma-Aldrich).

Immunohistochemistry and immunofluorescence

Single cells were plated on precoated poly-l-lysine coverslips and fixed in 1% paraformaldehyde for 10 min, rinsed with phosphate-buffered saline solution (PBS) at least three times, blocked in 10% goat serum with 0.2% Triton X-100 for 1 h, and washed at least three times with PBS and 0.2% Triton X-100. Brain tissues were fixed in 4% paraformaldehyde for 24 h, embedded in paraffin, sectioned serially (4 μm), and stained with hematoxylin and eosin (H&E; Sigma-Aldrich). For immunohistochemical staining, slides were deparaffinized and subjected to graded rehydration. After blocking in 5% serum and antigen retrieval citrate buffer (pH 6.0), the slides were incubated with the primary antibodies overnight at 4°C. After the slides were washed in PBS with Tween 20, the primary antibody reactions were detected by using a Vectastain ABC Kit (Vector Laboratories) with the respective secondary antibody. For immunofluorescence studies, tissue sections, after blocking, were incubated with an antibody overnight at 4°C, then with secondary antibody (Invitrogen) for 1 h at room temperature. Antibodies used included F4/80 (cat. #14–4801; eBioscience), POSTN (cat. #49480 [Santa Cruz Biotechnology]; cat. #Ap11962b [Abgent]), nestin (cat. #Ab6142 [Abcam]; cat. #2027 [Santa Cruz Biotechnology]), TGF beta1 (cat. #ab64715; Abcam), and HIF1 alpha (cat. #610958; BD Biosciences).

Invasion assay

A Matrigel basement membrane matrix (BD Biosciences) was used to conduct *in vitro* cell invasion assays. Transwell inserts in 24-well plates were coated with diluted Matrigel, and

cells were added to the transwells in triplicate. The cells (2×10^4/200 μL), with specific antibody (mouse IgG, integrin β1 AB cat. #MAB17781 [R&D Systems] or integrin β3 AB cat. #MAB3050 [R&D Systems]), were added to the upper part of each well. Serum-free medium containing recombinant TGF beta1 or POSTN was added to the bottom of each well. Plates were incubated at 37°C, and the transwell filters were fixed and stained with 0.1% crystal violet in 20% methanol. Invasive cells were visualized using bright-field microscopy. Transwell membranes were then incubated with 2% deoxycholic acid for 20 minutes, and the absorbance of invaded cells at 595 nm was recorded.

Enzyme-linked immunosorbent assays

Cell culture supernatants were collected and concentrations of VEGF-A and POSTN determined by human VEGF-A–specific (R&D Systems) and POSTN-specific (RayBiotech) enzyme-linked immunosorbent assay (ELISA) kits according to the manufacturers' instructions. Mean concentrations were recorded in picograms per milliliter.

Detection of multiple signaling pathways using Reverse Phase Protein Array

We used reverse-phase protein array analysis (RPPA) to detect activated signaling pathways in GSCs and gliomas extracted from mice. Cells and tissues were prepared for RPPA analysis by recommended protocols, and samples were probed with 218 and 166 validated primary antibodies, respectively, at the MD Anderson Functional Proteomics Reverse Phase Protein Array Core facility.

Statistical analysis

Unless otherwise noted, all reported results are from three independent experiments performed in triplicate. All statistical analyses were conducted by the InStat software program for Microsoft Windows (GraphPad Software). Data are reported as the mean ± standard deviation. Survival was analyzed by the Kaplan-Meier method. Tumor volumes among groups were compared using the log-rank test. All other data were compared by the unpaired two-tailed Student *t*-test.

Results

Glioma resistance to anti-VEGF-A therapy is associated with POSTN expression

A previous study found that anti-VEGF-A therapy induced increases in invasive characteristics in both GSC11 and U87 murine tumors while increasing median overall host survival (27). In the present study, we investigated the relationship between POSTN expression and bevacizumab resistance in murine bearing GSCs. In our previous model of anti-VEGF-A resistance (27), murine GSC11 and U87 tumors treated with bevacizumab expressed higher POSTN levels than control tumors (Figure 1A). We therefore examined the effect of POSTN *in vivo* on response to anti-VEGF-A therapy in mice. The median survival duration in animals implanted with control GSC272 cells was 70 days; median survival in animals implanted with GSC272 cells and treated with bevacizumab was 93 days; and median survival in animals implanted with POSTN-knockdown #1 and #2 GSC272 were 85 and 97 days, respectively (Figure 1B). As expected, and consistently with a previous study (28), bevacizumab-based treatment resulted in much longer survival durations than in

control mice. Moreover, knockdown of POSTN expression increased survival durations than in treatment with bevacizumab. Interestingly, the combination of POSTN knockdown and treatment with bevacizumab increased the median survival duration from 70 days to 100.5 (shRNA #1) and 115 (shRNA#2) days, respectively. After 7 weeks of treatment, the mean tumor volume in mice treated with bevacizumab (0.05 mm^3) and that in mice given POSTN shRNA-infected GSC272 cells (shRNA#1: 1.35; shRNA#2: 1.5 mm^3) were smaller than in control mice (9.63 mm^3). However, the group given POSTN shRNA GSC272 cells and treated with bevacizumab had no tumors (Figure 1C). After 17 weeks of treatment, only the mice given this combination were still alive (Figure 1B). At 16 weeks, the mean tumor volume in mice given the combination (shRNA#1: 30.79; shRNA#2: 25.65 mm^3) was lower than those in the mice treated with bevacizumab (100 mm^3) or POSTN shRNA GSC272 cells (shRNA#1: 70.35; shRNA#2: 61.06 mm^3). In mice implanted with GSC11 cells, those given the combination of POSTN-knockdown GSC11 cells with bevacizumab treatment had lower tumor volumes than the mice implanted with parental GSC11 cells given bevacizumab ($P < 0.01$; Supplementary Figure S1A). In particular, the mean number of nestin-positive cells in mice given POSTN shRNA-infected GSC11 cells alone or POSTN shRNA following bevacizumab were lower than those in the control and bevacizumab-treated mice (Supplementary Figure S1B). Immunohistochemical staining of GSC272 tumor samples found that POSTN expression was much higher in bevacizumab-treated mice than in control mice. POSTN expression was not detectable in mice given POSTN shRNA-infected GSCs regardless of bevacizumab treatment (Figure 1D).

POSTN expression in GSCs regulates TGF beta1 expression in macrophages

To determine the location of the expression of POSTN in GSCs relative to that in macrophages, we double-stained the stem cell marker nestin or the macrophage marker F4/80. We observed that POSTN was double-stained with nestin but not with F4/80 (Figure 2A; Supplementary Figure S2A). Others have found that TGF beta1 promoted the glioma mesenchymal phenotype and that its expression was markedly increased in a bevacizumab-resistant GSC cell line (10). Treatment with bevacizumab in the present study increased TGF beta1 expression in murine GSC272 and GSC11 xenografts (Figure 2B; Supplementary Figure S2B). The groups given both POSTN shRNA-infected GSCs and the combination of POSTN shRNA and bevacizumab did not have TGF beta1 expression. TGF beta1–expressing murine GSC272 tumors treated with bevacizumab exhibited double-staining for F4/80 (Figure 2C). In addition, expression of HIF1 alpha, a key regulator of resistance to anti-VEGF-A therapy, was lower in the POSTN shRNA groups than in the control (Figure 2D). These findings demonstrate that POSTN was expressed in GSCs and regulated the expression of TGF beta1 and HIF1 alpha during anti-VEGF-A therapy.

Expression of POSTN regulates invasion and VEGF-A expression in GSCs

To investigate the regulation of POSTN expression in GSCs, we performed Western blot analyzed the POSTN expression of several GSC lines. Expression of POSTN was highest in GSC6–27, GSC11, and GSC272 cells (Figure 3A). Stable knockdown of POSTN expression by the shRNA1, 2 and negative shRNA construct in GSCs abrogated POSTN expression (Supplementary Figure S3A). We compared the EMT and angiogenesis profiles of vector- and POSTN shRNA#2-infected GSC272 cells using a PCR-based arrays (Supplementary

Figure S3B). The results of this analysis are summarized in Supplementary Table 1. To expand on these findings, we performed VEGF-A ELISA and invasion assays. As shown in Figure 3B, VEGF-A expression decreased in POSTN shRNA-infected GSC272 cells. Also, POSTN shRNA infection decreased invasion of both GSC11 and GSC272 cells (Figure 3B; Supplementary Figure S3C). HIF1 alpha is key regulation factor for VEGF-A, so we performed an analysis of expression of HIF1alpha and phosphorylation of STAT3 in GSCs. Consistent with VEGF-A expression, expression of HIF1 alpha and phosphorylation of STAT3 decreased following knockdown of POSTN expression (Figure 3C). EMT related genes, N-cadherin and caveolin-1 expression were decreased by POSTN knockdown (Supplementary Figure S3D). To elucidate the role of STAT3 in POSTN regulation, we examined the effect of a STAT3 inhibitor (AZD1480) on HIF1 alpha and caveolin-1 expression. Treatment with the STAT3 inhibitor decreased levels of HIF1 alpha, VEGF-A, and caveolin-1 compared to control treatment (Supplementary Figure S3E). Also, expression of POSTN in GSC272 was decreased by the STAT3 inhibitor.

TGF beta1 increase POSTN secretion and downstream signaling

Growth factors such as TGF beta, EGF, and hepatocyte growth factor activate EMT (29–32), and primary lung fibroblasts upregulate POSTN expression in response to TGF beta3 and TGF beta2 (15). To identify the mechanism underlying regulation of POSTN expression by TGF beta1, we treated GSC272 cells with TGF beta1. TGF beta1 increased the secretion of POSTN and phosphorylation of SMAD3 (Figure 4A) and SMAD2 (Supplementary Figure S4A). After treatment with TGF beta1, secretion of POSTN increased greatly at 1 and 24 h. Also, secretion of POSTN was blocked by an inhibitor of TGF beta1 receptor with or without TGF beta1 stimulation (Supplementary Figure S4A). We found, furthermore, that TGF beta1 increased the expression of HIF1 alpha, VEGF-A, and STAT3 in GSC272 and the invasion via POSTN (Figure 4B and 4C; Supplementary Figure S4B).

Recombinant TGF beta1 and POSTN stimulate GSC invasion via integrin β1

Integrins influence cells' interaction with POSTN. Therefore, we characterized several integrin receptors in GSC lines. GSC11 cells expressed integrin β1 and integrin β3, whereas GSC272 cells expressed only integrin β1 (Figure 5A). In our evaluation of the role of the integrin β1 and integrin β3 receptors in POSTN expression, an anti-integrin β1 antibody blocked invasion induced by recombinant TGF beta1 and POSTN, whereas integrin β3 had no effect on invasion (Figure 5B; Supplementary Figure S5). Furthermore, recombinant POSTN stimulated phosphorylation of STAT3 and expression of caveolin-1. POSTN knockdown decreased expression of STAT3 and caveolin-1 protein induced by recombinant POSTN (Figure 5C).

Identification of POSTN-regulated genes in vitro and in vivo

To examine other potential markers of response of GSCs to POSTN, we used microarray analysis and RPPA. Differential mRNA expression patterns were seen in GSC272-vector compared to GSC272-POSTN shRNA tumors (Supplementary Figure S6). Likewise, RPPA data demonstrated that expression levels of pAKT (pT308, pS473), pS6 (S235, S236 and S240, S244), caveolin-1, collagen VI, annexin I, pGSK3AB (S21 and S9), IGFBP2, and pSTAT3 (Y705) proteins were significantly lower in POSTN-knockdown GSC272 cells than

in GSC272 control cells (Figure 6A). Furthermore, the expression of pS6 (S235, S236 and S240, S244), cyclin B1, TFRC, MEK1, caveolin-1, YB1, and VEGFR2 proteins was markedly lower in POSTN-knockdown GSC272 murine glioma samples than in control glioma samples (Figure 6A). In both cell lines and tumors from mice, caveolin-1 and pSTAT3 level were decreased by POSTN shRNA. We also examined the protein expression in a murine tumor sample *in vivo*, expression of caveolin-1, pSTAT3, POSTN, and HIF1 alpha was lower in a POSTN shRNA GSC272–derived mouse tumor than in a parental GSC272-derived mouse tumor (Figure 6B). Genes identified as regulated by POSTN both *in vitro* and *in vivo* were subjected to Ingenuity Pathway Analysis (QIAGEN) (Figure 6C).

Discussion

This is the first demonstration that knockdown of POSTN decreases resistance to anti-VEGF-A therapy in human GSCs *in vivo*. POSTN and VEGF-A are strongly associated with GSC progression. A previous study demonstrated that POSTN expression correlated directly with tumor grade and recurrence and inversely with survival at all grades of adult human glioma (17). We showed that POSTN was expressed in GSC6–27, GSC11, and GSC272 cells. Also, mice implanted with GSC11 and GSC272 cells increased POSTN expression by treatment with bevacizumab. Knockdown of POSTN decreased tumor growth and prolonged mouse survival as effectively as treatment with bevacizumab. Mice implanted with GSCs infected with POSTN shRNA and treated with bevacizumab exhibited a synergistic effect on tumor volume and survival.

The transforming growth factor beta induced (TGFBI; BIGH3) protein and POSTN have the same EMI domain and four highly conserved fasciclin I domains. However, they have different C-terminal domains; TGFBI has the RGD motif, whereas POSTN has a more extended C-terminal domain. TGFBI can bind with ECM (33) and POSTN (34). In addition, the C-terminal domain of POSTN binds to the ECM protein to regulate organization of the cellular matrix (35). GSCs have expression of POSTN but not TGFBI (data not shown). Therefore, the C-terminal domain of POSTN may be a key domain for GSC invasion.

In our PCR-based array experiment, POSTN influenced the expression of several angiogenesis- and EMT-related genes in GSC272 cells. Specifically, VEGF-A expression was lower in cells with knockdown of POSTN expression than in control cells. Also, HIF1 alpha activates transcription of various hypoxia-inducible genes, such as VEGF-A, and ECM metabolism (urokinase-type plasminogen activator receptor and MMPs) (36). We found that POSTN affected HIF1 alpha. Furthermore, MMP3 and MMP9 expression was lower in GSC272 cells with POSTN knockdown than in control cells in our PCR array. Additionally, EMT plays a critical role in invasiveness of cancer cells, and during EMT, cancer cells regulate expression of mesenchymal genes such as vimentin, fibronectin, MMPs, and N-cadherin. As an ECM protein, POSTN regulates cell adhesion (37). In pancreatic tumor cells, POSTN induces their invasiveness by downregulating E-cadherin expression via Snail (38). In our study, recombinant POSTN increased the invasiveness of GSC272 and GSC11 cells. Knockdown of POSTN expression resulted in less invasion and lower expression of the EMT-related genes N-cadherin and caveolin. It has been reported previously that caveolin-1 expression was downregulated in the cores and penumbrae of ischemic rat brains

(39). In another study, caveolin-1 affected VEGF, p42/44 MAPK, PI3K/AKT, and STAT3 signaling in neural progenitor stem cells (40). Finally, the STAT3 pathway is a potent regulator of the hypoxic pathway, and the STAT3 inhibitor AZD1480 may circumvent the induction of hypoxia in GBM (41). More interestingly, POSTN expression can be regulated by STAT3. We observed that treatment with AZD1480 abolished the expression of POSTN as well as HIF1 alpha, VEGF-A, and caveolin-1 in GSC272. Also, recombinant POSTN phosphorylated STAT3. Collectively, these results suggest that POSTN and STAT3 are controlled interactively. Studies elucidating the mechanisms of caveolin-related invasion in glioma are being planned.

We found that TGF beta1 increased the secretion of POSTN, which regulates several EMT and angiogenesis markers *in vitro*. In a previous study, TGF beta1 induced ECM proteins involved in cell survival, angiogenesis, and invasion (12). In another, POSTN decreased HIF1 alpha accumulation by blocking TGF beta1 type I receptor signaling in human PDL cells *in vitro* (42). Here we observed that, in GSC cells, POSTN secretion was increased by TGF beta1 and blocked by treatment with an inhibitor of the TGF beta receptor. After treatment with TGF beta1, phosphorylation of SMAD3 and SMAD2 increased in GSC272 cells. POSTN appears to be a key regulator of TGF beta1–induced invasion and VEGF-A expression, and TGF beta1 increases the expression of HIF1 alpha.

The expression of the αvβ3 and αvβ5 integrin heterodimer subtypes correlates directly with glioma grade (43). Ishida et al. (44) reported that an antagonist of integrin αvβ3 and integrin αvβ5 prevented bevacizumab-induced invasion in orthotopic glioma models that express these integrins at high levels. We found that GSC11 cells expressed the POSTN receptors integrin β1 and integrin β3 and that GSC272 cells expressed integrin β1 more highly than integrin β3. Exposure to an antibody against integrin β1 blocked invasiveness induced by TGF beta1 and POSTN in GSC11 and GSC272 cells but integrin β3 did not.

GBM is a highly vascularized tumor, and VEGF-A is a key regulator of tumor angiogenesis. In animal models, bevacizumab inhibits angiogenesis and tumor growth (45). Anti-VEGF therapy alone results in resistance, including increased expression of growth factors, angiopoietin1, VEGF, stromal cell-derived factor-1A, stem cell factors, STAT3, and osteopontin (46–49). Several factors are induced by hypoxia and increased HIF1 alpha protein expression. We know that TGF beta expression in GSC11 cells is increased by bevacizumab-based treatment in mice (10), but the mechanism of its regulation has yet to be determined. In mice implanted with POSTN shRNA-infected GSC272 cells, resistance to bevacizumab-based treatment decreased the expression of both HIF1 alpha and TGF beta1. During tumor growth in mice, POSTN was expressed in GSCs while TGF beta1 was expressed by macrophages. Anti-VEGF-A therapy is known to increase the infiltration of macrophages (50). After inflammation or mechanical stress, expression of TGF beta1 increases in macrophages and neutrophils (37). Our results demonstrate that treatment with bevacizumab increased POSTN expression in GSCs, which mediates TGF beta1 expression in macrophages. Malanchi *et al.* (15) reported that POSTN functions as a bridge between cancer stem cells and their metastatic niches. Evidence reported herein suggests that POSTN regulates interaction between GSCs and their environment during anti-VEGF-A therapy.

Targeting POSTN may represent a novel method to overcome the highly infiltrative phenotype of GBM and prevent resistance to antiangiogenic therapy.

Supplementary Material

Refer to Web version on PubMed Central for supplementary material.

Acknowledgments

The authors thank Kay Hyde and Kathryn Hale for editorial assistance.

Financial Support: This work was supported in part by the M. G. Williams Memorial Brain Tumor Research Fund (J.F. de Groot) and NCI Cancer Center Support Grant (P30 CA016672, R.A. DePinho).

Abbreviations

POSTN	Periostin
EMT	Epithelial-to-mesenchymal transition
VEGF-A	Vascular endothelial growth factor A
TGF beta1	Transforming growth factor beta-1
HIF1 alpha	Hypoxia-inducible factor-1 alpha
STAT3	Signal transducer and activator of transcription 3
GBM	Glioblastoma
GSCs	Glioma stem cells
ECM	Extracellular matrix
shRNA	short hairpin RNA
bFGF	Basic fibroblast growth factor
EGF	Epidermal growth factor
PBS	Phosphate-buffered saline solution
RPPA	Reverse-phase protein array
ELISA	Enzyme-linked immunosorbent assay
PCR	Polymerase chain reaction
H&E	Hematoxylin and eosin
TGFBI	Transforming growth factor beta induced

References

1. Arrillaga-Romany I, Reardon DA, Wen PY. Current status of antiangiogenic therapies for glioblastomas. Expert Opin Investig Drugs. 2014; 23:199–210.
2. Liu LX, Lu H, Luo Y, Date T, Belanger AJ, Vincent KA, et al. Stabilization of vascular endothelial growth factor mRNA by hypoxia-inducible factor 1. Biochem Biophys Res Commun. 2002; 291:908–914. [PubMed: 11866451]
3. Bao S, Wu Q, Sathornsumetee S, Hao Y, Li Z, Hjelmeland AB, et al. Stem cell-like glioma cells promote tumor angiogenesis through vascular endothelial growth factor. Cancer Res. 2006; 66:7843–7848. [PubMed: 16912155]
4. Takano S, Yoshii Y, Kondo S, Suzuki H, Maruno T, Shirai S, et al. Concentration of vascular endothelial growth factor in the serum and tumor tissue of brain tumor patients. Cancer Res. 1996; 56:2185–2190. [PubMed: 8616870]
5. Soda Y, Myskiw C, Rommel A, Verma IM. Mechanisms of neovascularization and resistance to anti-angiogenic therapies in glioblastoma multiforme. J Mol Med. 2013; 91:439–448. [PubMed: 23512266]
6. Leon SP, Folkerth RD, Black PM. Microvessel density is a prognostic indicator for patients with astroglial brain tumors. Cancer. 1996; 77:362–372. [PubMed: 8625246]
7. Phillips HS, Kharbanda S, Chen R, Forrest WF, Soriano RH, Wu TD, et al. Molecular subclasses of high-grade glioma predict prognosis, delineate a pattern of disease progression, and resemble stages in neurogenesis. Cancer Cell. 2006; 9:157–173. [PubMed: 16530701]
8. Ferrara N, Hillan KJ, Gerber HP, Novotny W. Discovery and development of bevacizumab, an anti-VEGF antibody for treating cancer. Nat Rev Drug Discov. 2004; 3:391–400. [PubMed: 15136787]
9. de Groot JF, Fuller G, Kumar AJ, Piao Y, Eterovic K, Ji Y, et al. Tumor invasion after treatment of glioblastoma with bevacizumab: radiographic and pathologic correlation in humans and mice. Neuro Oncol. 2010; 12:233–242. [PubMed: 20167811]
10. Piao Y, Liang J, Holmes L, Henry V, Sulman E, de Groot JF. Acquired resistance to anti-VEGF therapy in glioblastoma is associated with a mesenchymal transition. Clin Cancer Res. 2013; 19:4392–4403. [PubMed: 23804423]
11. Norris RA, Potts JD, Yost MJ, Junor L, Brooks T, Tan H, et al. Periostin promotes a fibroblastic lineage pathway in atrioventricular valve progenitor cells. Dev Dyn. 2009; 238:1052–1063. [PubMed: 19334280]
12. Kim JE, Kim SJ, Lee BH, Park RW, Kim KS, Kim IS. Identification of motifs for cell adhesion within the repeated domains of transforming growth factor-beta-induced gene, betaig-h3. J Biol Chem. 2000; 275:30907–30915. [PubMed: 10906123]
13. Politz O, Gratchev A, McCourt PA, Schledzewski K, Guillot P, Johansson S, et al. Stabilin-1 and −2 constitute a novel family of fasciclin-like hyaluronan receptor homologues. Biochem J. 2002; 362:155–164. [PubMed: 11829752]
14. Takeshita S, Kikuno R, Tezuka K, Amann E. Osteoblast-specific factor 2: cloning of a putative bone adhesion protein with homology with the insect protein fasciclin I. Biochem J. 1993; 294:271–278. [PubMed: 8363580]
15. Malanchi I, Santamaria-Martinez A, Susanto E, Peng H, Lehr HA, Delaloye JF, et al. Interactions between cancer stem cells and their niche govern metastatic colonization. Nature. 2012; 481:85–89.
16. Wang H, Wang Y, Jiang C. Stromal protein periostin identified as a progression associated and prognostic biomarker in glioma via inducing an invasive and proliferative phenotype. Int J Oncol. 2013; 42:1716–1724. [PubMed: 23467707]
17. Mikheev AM, Mikheeva SA, Trister AD, Tokita MJ, Emerson SN, Parada CA, et al. Periostin is a novel therapeutic target that predicts and regulates glioma malignancy. Neuro Oncol. 2015; 17:372–382. [PubMed: 25140038]
18. Butcher JT, Norris RA, Hoffman S, Mjaatvedt CH, Markwald RR. Periostin promotes atrioventricular mesenchyme matrix invasion and remodeling mediated by integrin signaling through Rho/PI 3-kinase. Dev Biol. 2007; 302:256–266. [PubMed: 17070513]

19. Nuzzo PV, Buzzatti G, Ricci F, Rubagotti A, Argellati F, Zinoli L, et al. Periostin: a novel prognostic and therapeutic target for genitourinary cancer? Clin Genitourin Cancer. 2014; 12:301–311. [PubMed: 24656869]
20. Yan W, Shao R. Transduction of a mesenchyme-specific gene periostin into 293T cells induces cell invasive activity through epithelial-mesenchymal transformation. J Biol Chem. 2006; 281:19700–19708. [PubMed: 16702213]
21. Kudo Y, Iizuka S, Yoshida M, Nguyen PT, Siriwardena SB, Tsunematsu T, et al. Periostin directly and indirectly promotes tumor lymphangiogenesis of head and neck cancer. PLoS One. 2012; 7:e44488. [PubMed: 22952986]
22. Horiuchi K, Amizuka N, Takeshita S, Takamatsu H, Katsuura M, Ozawa H, et al. Identification and characterization of a novel protein, periostin, with restricted expression to periosteum and periodontal ligament and increased expression by transforming growth factor beta. J Bone Miner Res. 1999; 14:1239–1249. [PubMed: 10404027]
23. Ji X, Chen D, Xu C, Harris SE, Mundy GR, Yoneda T. Patterns of gene expression associated with BMP-2-induced osteoblast and adipocyte differentiation of mesenchymal progenitor cell 3T3-F442A. J Bone Miner Metab. 2000; 18:132–139. [PubMed: 10783846]
24. Tada T, Yabu K, Kobayashi S. Detection of active form of transforming growth factor-beta in cerebrospinal fluid of patients with glioma. Jpn J Cancer Res. 1993; 84:544–548. [PubMed: 8320172]
25. Leitlein J, Aulwurm S, Waltereit R, Naumann U, Wagenknecht B, Garten W, et al. Processing of immunosuppressive pro-TGF-beta 1,2 by human glioblastoma cells involves cytoplasmic and secreted furin-like proteases. J Immunol. 2001; 166:7238–7243. [PubMed: 11390472]
26. Singh SK, Hawkins C, Clarke ID, Squire JA, Bayani J, Hide T, et al. Identification of human brain tumour initiating cells. Nature. 2004; 432(7015):396–401. [PubMed: 15549107]
27. Piao Y, Liang J, Holmes L, Zurita AJ, Henry V, Heymach JV, et al. Glioblastoma resistance to anti-VEGF therapy is associated with myeloid cell infiltration, stem cell accumulation, and a mesenchymal phenotype. Neuro Oncol. 2012; 14:1379–1392. [PubMed: 22965162]
28. Lucio-Eterovic AK, Piao Y, de Groot JF. Mediators of glioblastoma resistance and invasion during antivascular endothelial growth factor therapy. Clin Cancer Res. 2009; 15:4589–4599. [PubMed: 19567589]
29. Kim K, Lu Z, Hay ED. Direct evidence for a role of beta-catenin/LEF-1 signaling pathway in induction of EMT. Cell Biol Int. 2002; 26:463–476. [PubMed: 12095232]
30. Davies M, Robinson M, Smith E, Huntley S, Prime S, Paterson I. Induction of an epithelial to mesenchymal transition in human immortal and malignant keratinocytes by TGF-beta1 involves MAPK, Smad and AP-1 signalling pathways. J Cell Biochem. 2005; 95:918–931. [PubMed: 15861394]
31. Nawshad A, Lagamba D, Polad A, Hay ED. Transforming growth factor-beta signaling during epithelial-mesenchymal transformation: implications for embryogenesis and tumor metastasis. Cells Tissues Organs. 2005; 179:11–23. [PubMed: 15942189]
32. Hardy KM, Booth BW, Hendrix MJ, Salomon DS, Strizzi L. ErbB/EGF signaling and EMT in mammary development and breast cancer. J J Mammary Gland Biol Neoplasia. 2010; 15:191–199. [PubMed: 20369376]
33. Hashimoto K, Noshiro M, Ohno S, Kawamoto T, Satakeda H, Akagawa Y, et al. Characterization of a cartilage-derived 66-kDa protein (RGD-CAP/beta ig-h3) that binds to collagen. B Biochim Biophys Acta. 1997; 1355:303–314.
34. Kim BY, Olzmann JA, Choi SI, Ahn SY, Kim TI, Cho HS, et al. Corneal dystrophy-associated R124H mutation disrupts TGFBI interaction with Periostin and causes mislocalization to the lysosome. J Biol Chem. 2009; 284:19580–19591. [PubMed: 19478074]
35. Hoersch S, Andrade-Navarro MA. Periostin shows increased evolutionary plasticity in its alternatively spliced region. BMC Evol Biol. 2010; 10:30. [PubMed: 20109226]
36. Semenza GL. Targeting HIF-1 for cancer therapy. Nat Rev Cancer. 2003; 3:721–732. [PubMed: 13130303]

37. Takayama G, Arima K, Kanaji T, Toda S, Tanaka H, Shoji S, et al. Periostin: a novel component of subepithelial fibrosis of bronchial asthma downstream of IL-4 and IL-13 signals. J Allergy Clin Immunol. 2006; 118:98–104. [PubMed: 16815144]
38. Kim CJ, Sakamoto K, Tambe Y, Inoue H. Opposite regulation of epithelial-to-mesenchymal transition and cell invasiveness by periostin between prostate and bladder cancer cells. Int J Oncol. 2011; 38:1759–1766. [PubMed: 21468544]
39. Shen J, Ma S, Chan P, Lee W, Fung PC, Cheung RT, et al. Nitric oxide down-regulates caveolin-1 expression in rat brains during focal cerebral ischemia and reperfusion injury. J Neurochem. 2006; 96:1078–1089. [PubMed: 16417587]
40. Temple S. The development of neural stem cells. Nature. 2001; 414:112–117. [PubMed: 11689956]
41. de Groot J, Liang J, Kong LY, Wei J, Piao Y, Fuller G, et al. Modulating antiangiogenic resistance by inhibiting the signal transducer and activator of transcription 3 pathway in glioblastoma. Oncotarget. 2012; 3:1036–1048. [PubMed: 23013619]
42. Aukkarasongsup P, Haruyama N, Matsumoto T, Shiga M, Moriyama K. Periostin inhibits hypoxia-induced apoptosis in human periodontal ligament cells via TGF-beta signaling. Biochem Biophys Res Commun. 2013; 441:126–132. [PubMed: 24129188]
43. Schnell O, Krebs B, Wagner E, Romagna A, Beer AJ, Grau SJ, et al. Expression of integrin alphavbeta3 in gliomas correlates with tumor grade and is not restricted to tumor vasculature. Brain Pathol. 2008; 18:378–386. [PubMed: 18394009]
44. Ishida J, Onishi M, Kurozumi K, Ichikawa T, Fujii K, Shimazu Y, et al. Integrin inhibitor suppresses bevacizumab-induced glioma invasion. Transl Oncol. 2014; 7:292–302. e1. [PubMed: 24704537]
45. Presta LG, Chen H, O'Connor SJ, Chisholm V, Meng YG, Krummen L, et al. Humanization of an anti-vascular endothelial growth factor monoclonal antibody for the therapy of solid tumors and other disorders. Cancer Res. 1997; 57:4593–4599. [PubMed: 9377574]
46. Batchelor TT, Sorensen AG, di Tomas oE, Zhang WT, Duda DG, Cohen KS, et al. AZD2171, a pan-VEGF receptor tyrosine kinase inhibitor, normalizes tumor vasculature and alleviates edema in glioblastoma patients. Cancer Cell. 2007; 11:83–95. [PubMed: 17222792]
47. Casanovas O, Hicklin DJ, Bergers G, Hanahan D. Drug resistance by evasion of antiangiogenic targeting of VEGF signaling in late-stage pancreatic islet tumors. Cancer Cell. 2005; 8:299–309. [PubMed: 16226705]
48. Fernando NT, Koch M, Rothrock C, Gollogly LK, D'Amore PA, Ryeom S, et al. Tumor escape from endogenous, extracellular matrix-associated angiogenesis inhibitors by up-regulation of multiple proangiogenic factors. Clin Cancer Res. 2008; 14:1529–1539. [PubMed: 18316578]
49. Ebos JM, Lee CR, Kerbel RS. Tumor and host-mediated pathways of resistance and disease progression in response to antiangiogenic therapy. Clin Cancer Res. 2009; 15:5020–5025. [PubMed: 19671869]
50. Liang J, Piao Y, Holmes L, Fuller GN, Henry V, Tiao N, et al. Neutrophils promote the malignant glioma phenotype through S100A4. Clin Cancer Res. 2014; 20:187–198. [PubMed: 24240114]

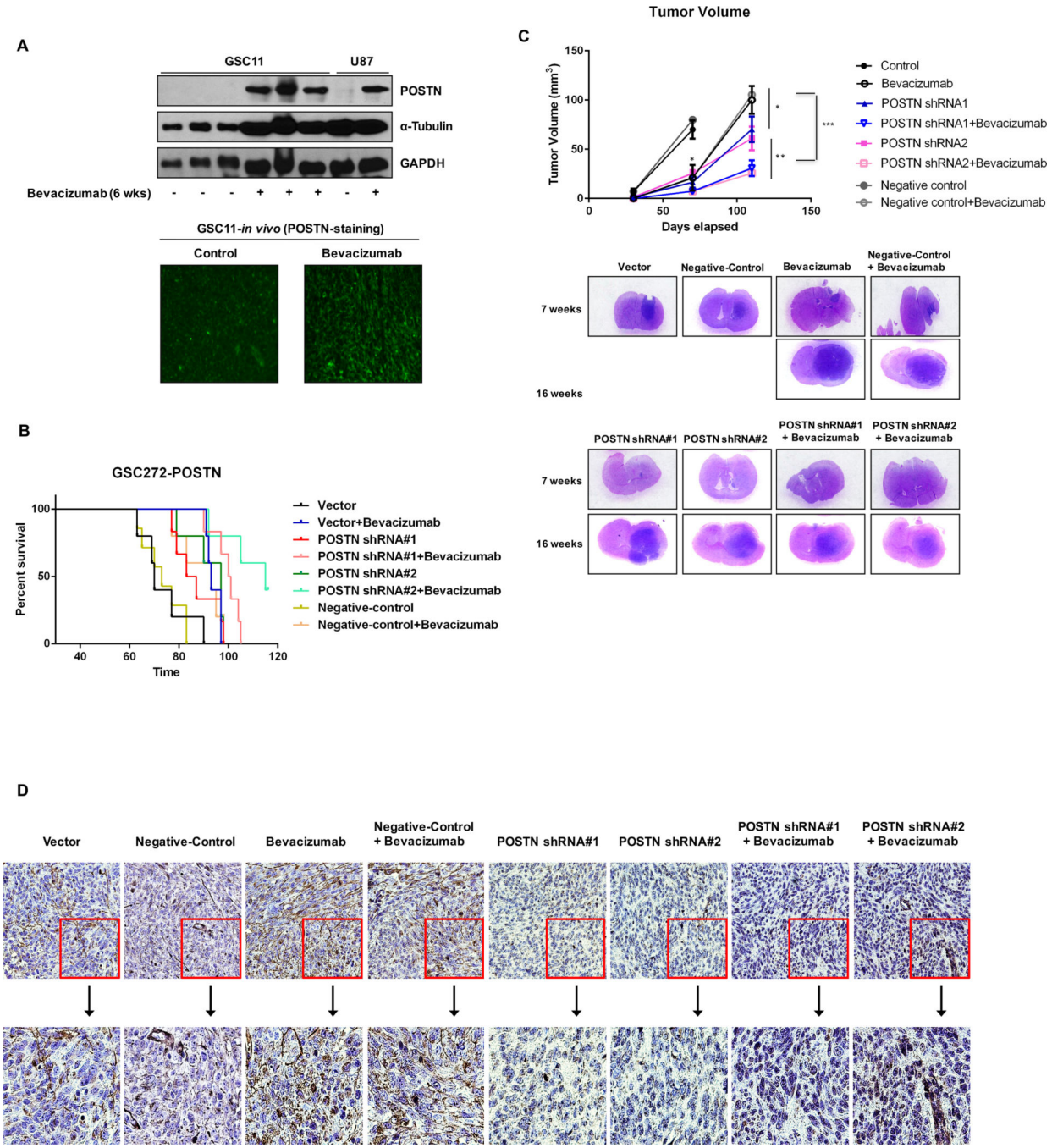

Figure 1.

Knockdown of POSTN expression prolongs survival and decreases tumor volume in glioma mouse models. (A) GSC11 and U87 cells were intracranially transplanted into the brains of mice (5×10^5 cells/mouse). Afterward, bevacizumab was administered via intraperitoneal injection. Proteins were collected from tumors (control group, at 4 weeks; bevacizumab group, at 6 weeks), and POSTN expression was detected by Western blot analysis. POSTN expression (green) was detected on frozen sections of mouse brain tumors by immunofluorescent staining. (B) The effects of POSTN knockdown and bevacizumab

treatment on GBM growth and survival were examined in a mouse intracranial xenograft model. GSC272 cells were infected with a lentivirus containing vector shRNA, POSTN shRNA#1, POSTN shRNA#2 or negative control shRNA and then intracranially transplanted into the brains of immunocompromised mice (5×10^5 cells/mouse). Tumors derived from POSTN-knockdown GSCs, with or without bevacizumab treatment, were harvested simultaneously and examined to determine the impact of disruption of POSTN expression. Survival of the study mice was estimated by the Kaplan-Meier method. In the GSC272 group, the following were compared: control versus treatment with bevacizumab ($P = 0.001$), control versus POSTN knockdown (#1: $P = 0.05$; #2: $P = 0.013$), POSTN knockdown versus POSTN knockdown plus treatment with bevacizumab (#1: $P = 0.01$; #2: $P = 0.002$), treatment with bevacizumab versus POSTN knockdown plus treatment with bevacizumab (#1: $P = 0.044$; #2: $P = 0.002$). (C) Murine brains harvested on day 30, 70, or 110 after transplantation of parental GSCs or POSTN-knockdown GSCs with or without treatment with bevacizumab were stained with H&E. At 70 days, treatment with bevacizumab and knockdown of POSTN expression resulted in smaller tumors than those in control mice ($*P < 0.05$). At 110 days, the combination resulted in smaller tumors than those in the bevacizumab-treated ($***P < 0.001$) and POSTN-knockdown ($**P < 0.01$) groups. (D) Immunohistochemical stains of GSC272 tumor samples for POSTN. POSTN-positive cells stained in nuclei.

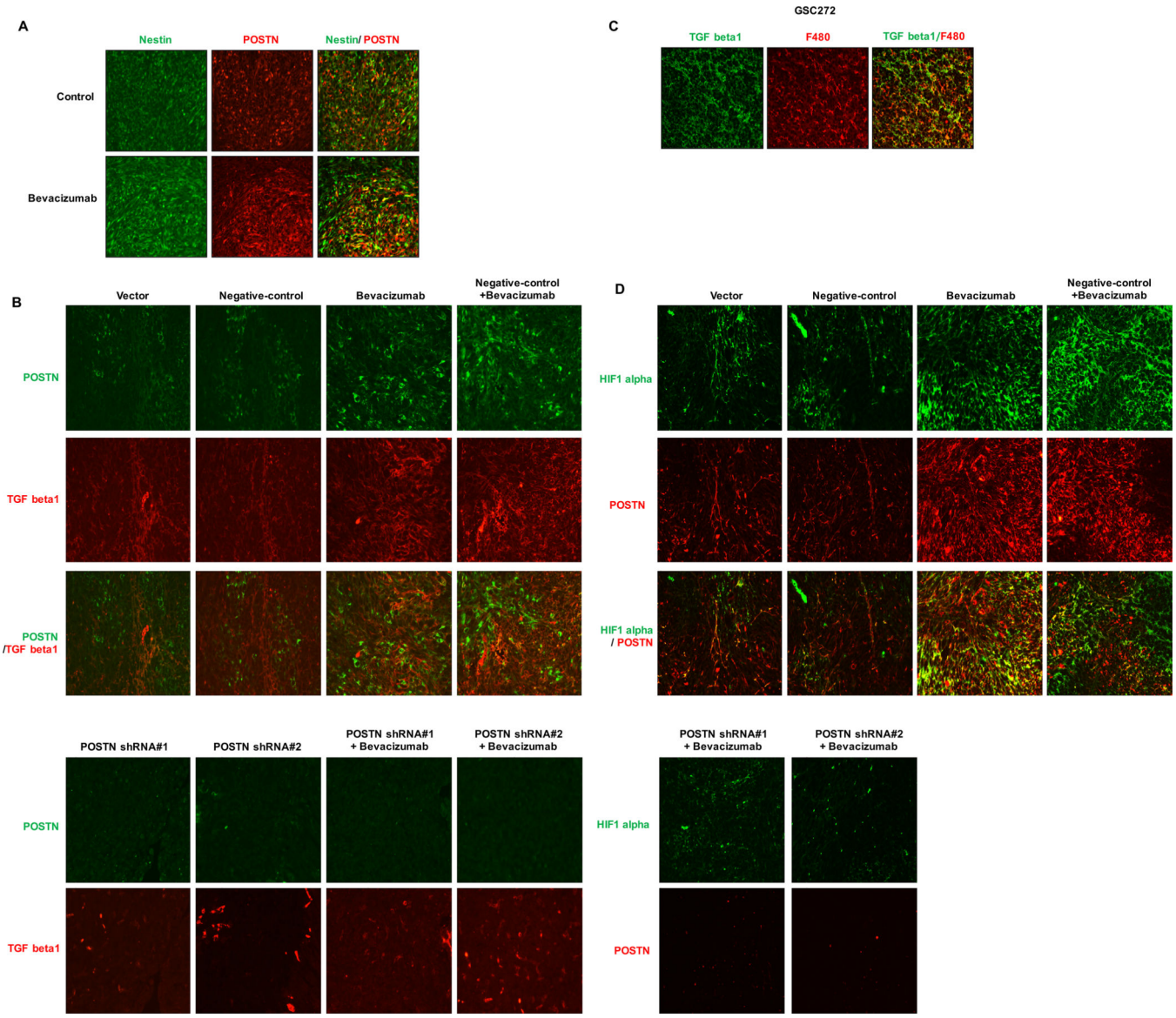

Figure 2.

Treatment with bevacizumab increases the expression of HIF1 alpha and TGF beta1 via POSTN. Immunofluorescent stains are shown for POSTN and the GSC markers nestin (A), TGF beta1 (B), and HIF1 alpha (C) in GSC272 mouse glioma xenografts with or without POSTN knockdown and/or treatment with bevacizumab. (A) Expression of POSTN (red) and of nestin (green) overlaps. (B) TGF beta1 (red) and POSTN (green) were expressed at different sites. (C) TGF beta1 (green) was expressed in F4/80-positive cells (red). (D) Immunofluorescent stains for POSTN (red) in relation to hypoxia marked by HIF1 alpha staining (green).

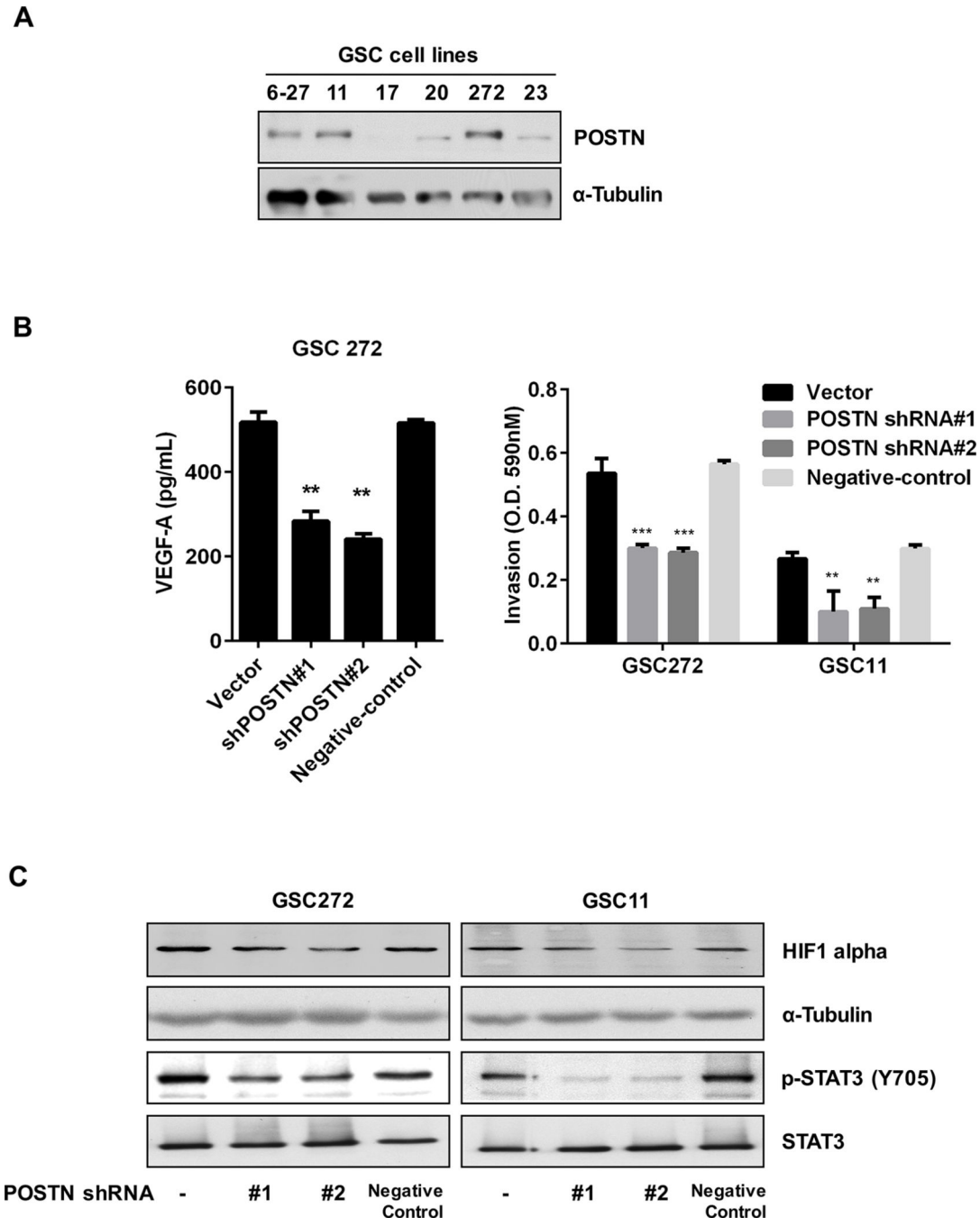

Figure 3.

POSTN regulates invasiveness and VEGF-A expression in GSCs. (A) GSC cell lysates were collected and analyzed for POSTN expression by Western blot. (B and C) GSC11 and GSC272 cells were infected with a lentivirus containing a control vector, POSTN shRNA or negative-control. (B) Expression of VEGF-A in the cells was measured by a VEGF-A ELISA kit. The invasiveness of GSCs (vector-, POSTN shRNA-infected or negative-control) was assessed by an invasion assay for 18 h. $^{**}P < 0.01$, $^{***}P < 0.001$ versus control. (C) Expression of HIF1 alpha and STAT3 in the GSCs was detected by Western blotting.

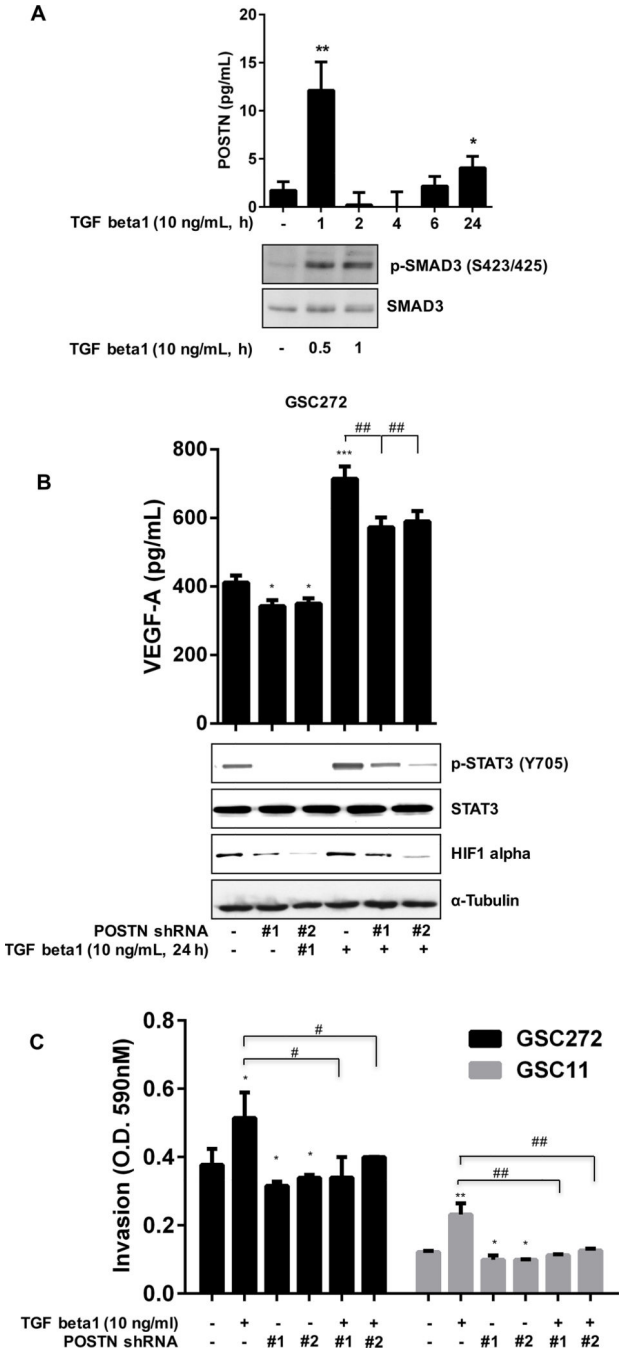

Figure 4.

TGF beta1 increases pSTAT3, HIF1 alpha, and VEGF-A expression in and invasiveness of GSCs. (A) GSC272 cells were seeded in 6-well plates for 24 h and treated with TGF beta1 (in medium without EGF or bFGF) for the indicated times. Secretion of POSTN and expression of SMAD3 in GSC272 cells were assessed by ELISA and Western blot analysis, respectively. *$P < 0.05$, **$P < 0.01$ versus control. (B) GSC272 cells infected with vector shRNA or POSTN shRNA were treated with TGF beta1 for 24 h; expression of VEGF-A was determined by ELISA and expression of p-STAT3, STAT3, and HIF1 alpha was

determined by Western blot. *$P < 0.05$, ***$P < 0.001$ versus control; ##$P < 0.01$ versus TGF beta1. (C) GSC272 cells infected with a vector or POSTN shRNA were added to the upper chambers of a transwell insert (2×10^4 cells/well), and medium containing recombinant TGF beta1 was added to the lower chambers; the plate was incubated for 18 h at 37°C. *$P < 0.05$, **$P < 0.01$ versus control; #$P < 0.05$, ##$P < 0.01$ versus TGF beta1.

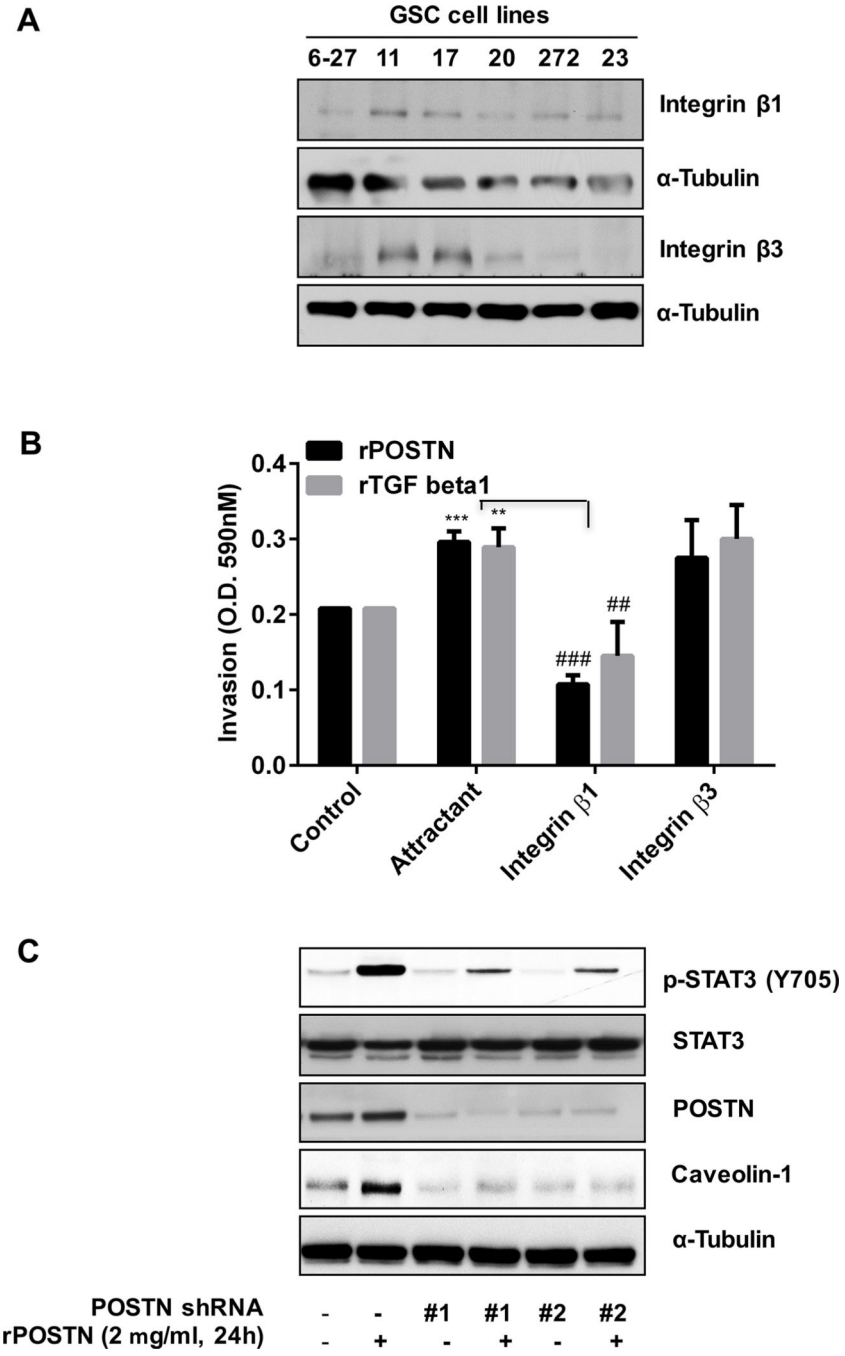

Figure 5.

Recombinant POSTN and TGF beta1 increase GSC invasiveness via integrin β1. (A) Expression of integrin β1 and integrin β3 proteins was measured in several GSC lines by Western blotting. (B) GSCs (2×10^4 cells/well) were rotated with antibody to integrin β1 or β3 for 1 h at room temperature, and cells were added to the upper chambers of a transwell insert plate. Medium containing recombinant POSTN or TGF beta1 was added to the lower chambers, and the plate was incubated for 18 h at 37°C. $^{**}P < 0.01$, $^{***}P < 0.001$ versus control; $^{\#\#}P < 0.01$, $^{\#\#\#}P < 0.001$ versus POSTN or TGF beta1. (C) Vector- and POSTN

shRNA-infected GSC272 cells were treated with 2 μg/mL recombinant POSTN for 24 h. Phosphorylation of STAT3 and expression of POSTN and caveolin-1 in the cells were assessed by Western blotting.

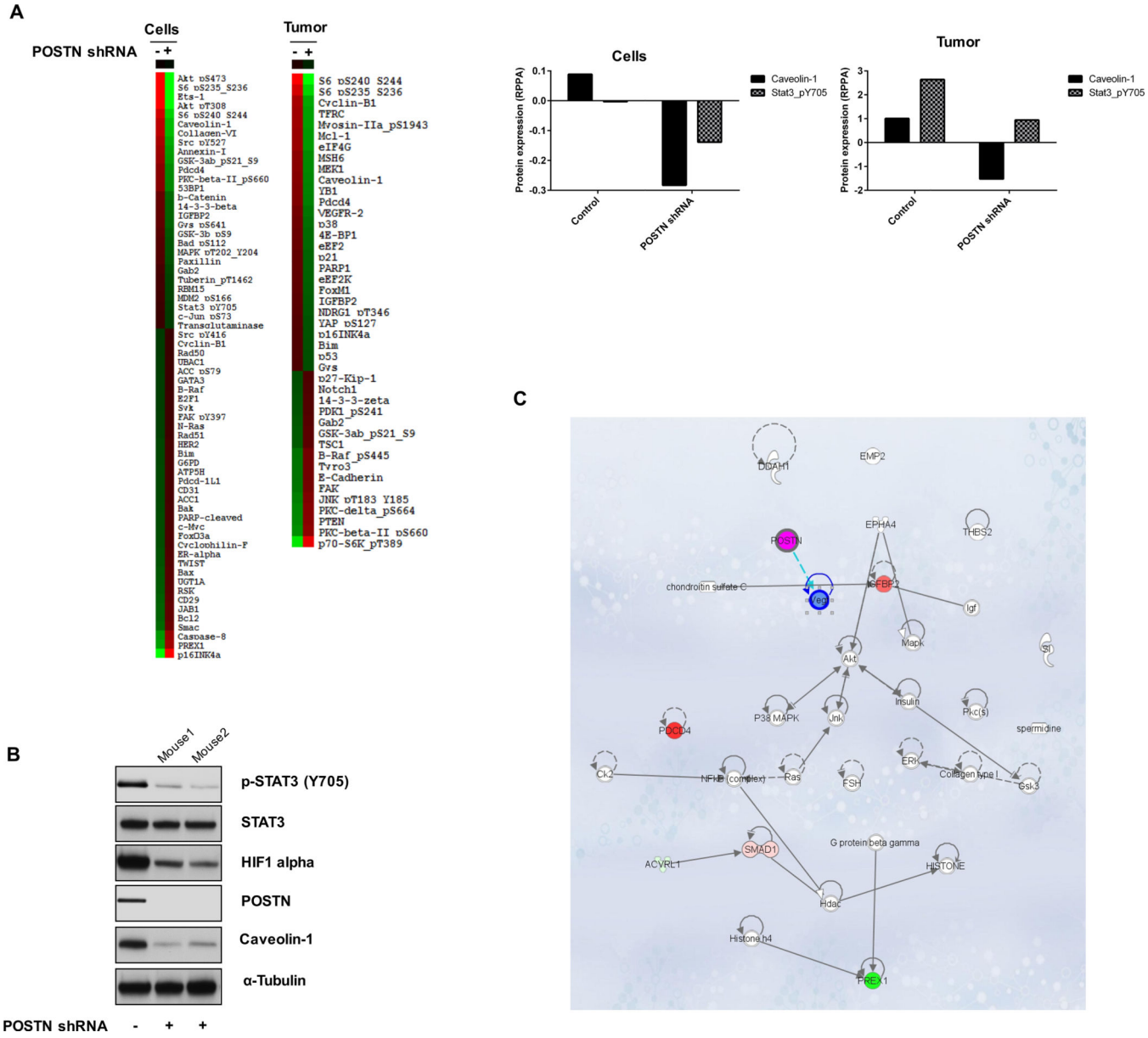

Figure 6.

Expression of proteins related to POSTN were quantified in GSCs and GSC-derived mouse tumors by RPPA. (A) Expression of various proteins was determined in GSC272 cells (vector- or POSTN shRNA-infected) and murine glioma samples derived from GSC272 (vector- or POSTN shRNA-infected) at 12 weeks after implantation. The protein expression levels in POSTN shRNA-infected cells and tumors that differed at least 1.3-fold (GSC272 cells) or 0.7-fold (murine glioma samples) from controls were selected for hierarchical clustering analysis. The red and green colors reflect relatively high and low expression, respectively. (B) Western blot analysis detected proteins expression in murine GSC272 glioma samples with and without POSTN knockdown. (C) Ingenuity Pathway Analysis

examined the intercellular signaling interaction network identified by *in vitro* and *in vivo* RPPA results.